The crucial role of temperature in atomic scale friction

2008 J. Phys.: Condens. Matter 20 354003

(http://iopscience.iop.org/0953-8984/20/35/354003)

J. Phys.: Condens. Matter **20** (2008) 354003 (7pp) doi:10.1088/0953-8984/20/35/354003

The crucial role of temperature in atomic scale friction

Sergey Yu Krylov[1,2] **and Joost W M Frenken**[1]

[1] Kamerlingh Onnes Laboratory, Leiden University, 2300 RA Leiden, The Netherlands
[2] Institute of Physical Chemistry and Electrochemistry, Russian Academy of Sciences, 119991 Moscow, Russia

E-mail: krylov@redline.ru and frenken@physics.LeidenUniv.nl

Received 27 April 2008
Published 11 August 2008
Online at stacks.iop.org/JPhysCM/20/354003

Abstract
The temperature dependence of atomic scale friction is analyzed theoretically, in the framework of a two-spring–two-mass generalization of the Prandtl–Tomlinson model, taking into account an ultra-low value of the effective mass of the contact. A decrease of the friction force with increasing temperature is predicted, that is unexpectedly strong, nontrivial in detail, and accompanied by transitions between different regimes of sliding corresponding to different scenarios of energy dissipation. The results indicate a much more pronounced role of thermally driven dynamics in friction than has ever been imagined, and they should strongly stimulate temperature-variable friction force microscopy experimentation.

1. Introduction

Should friction depend on temperature? Maybe yes, maybe no, depending on 'details' like spatial and temporal scales involved—this is the answer most expected to be given by a physicist or engineer. However, if we readdressed the question with respect to *atomic scale* friction, the expected answer would be rather certain and positive. Indeed, atomically small objects are known to be subject to intensive and variable thermal motion which is likely to affect dissipation.

It may seem surprising, but the two-decade developments of the science of nanotribology [1–4] have revealed only a very modest role of thermal effects in friction. Typical experimental observations (e.g. atomic stick–slip) are more or less easily explained by models (e.g. the Prandtl–Tomlinson model [5, 6]) which lead, at least in a first approximation, to temperature-independent results. Thermal effects manifested themselves in rather subtle observations, like weak, logarithmic dependence of friction force on velocity [7]. With very few exceptions [8], most friction force microscopy (FFM) experiments, the main tool for studying nanoscale friction [1], have been performed at room temperature, and so far there have been no very strong theoretical suggestions to perform temperature-variable experiments.

The main message of this paper is to show that, under many typical conditions, thermal effects play in fact dominant, if not crucial, roles, thus rehabilitating initial expectations of a naive physicist and strongly stimulating temperature-variable experimentation. The dependence of atomic scale friction on temperature is predicted to be nontrivial and physically rich. For certain values of the system parameters involved, even a very modest change of temperature can lead to an order-of-magnitude change in friction. At different temperatures one observes physically different regimes of sliding which correspond to essentially different scenarios of energy dissipation. Also nontrivial is the existence of stochastic regimes when the mean friction force strongly fluctuates, in spite of being averaged over a relatively large sliding distance passed over by the system. All these features are mainly concerned with an ultra-low value of the effective mass of the nanocontact [9] which thus can exhibit intensive thermally activated motion along the surface, including the cases of its partial or complete delocalization [10].

A detailed introduction to the problem, as well as a systematic analysis of the possible friction regimes, has been given in our recent paper [11]. Here we extend the previous work to the analysis of the temperature dependence of friction, and we start in the next section with just a brief discussion of the basic steps taken so far.

2. Effective mass of nanocontact and friction regimes

The friction force microscopy experiments are believed to provide direct, atomic scale access to the origin of

friction [1–4], since the FFM tip is thought to model the behavior of a single asperity, similar to one of the many asperities that make up the contact between two macroscopic sliding bodies. Experiments with atomic resolution usually demonstrate a periodic, sawtooth-like behavior of the lateral force, with the period of the substrate lattice. This is called atomic stick–slip (SS), reminiscent of the macroscale stick–slip which is responsible, for instance, for the noise of a creaky door or the voice of a violin. Atomic stick–slip is usually thought to be at the origin of friction. It is most easily explained using the traditional Prandtl–Tomlinson model [5, 6], which considers an object (the tip) moving in a periodic potential field formed by its interaction with the substrate lattice, being dragged along the surface by a rigid, external support, via a macroscopic spring (the cantilever), which is at the same time used to measure the lateral force experienced. Friction force is determined as the time average of the instantaneous lateral force. A remarkable result of the Prandtl–Tomlinson model is the prediction of a transition from stick–slip to continuous, near-frictionless sliding; the regime is often called superlubricity (SL). This transition takes place at a critically low value of the relative potential corrugation, with respect to the stiffness of the driving spring. The transition from SS to continuous sliding has been observed in recent experiments [12, 13].

In its simplest approximation, when one assumes complete dissipation of the excess of energy in each slip event, the Prandtl–Tomlinson model leads to temperature- and velocity-independent results for the friction force. Generalizations of the model, from dynamical modeling to nonequilibrium statistical mechanics [15–21], have advanced our understanding of atomic scale friction, in particular, a certain role of thermal effects has been revealed. Thus, thermal activation of the tip motion was understood to be responsible for a weak, logarithmic-like dependence of friction on scanning velocity, as first observed and explained in [7].

A basic problem, which has not been fully recognized yet, is concerned with flexibility of the FFM tip. At first glance, it seems a very hard object. However, the spring constant, directly measured in experiments, is usually much smaller than the stiffness K of the cantilever, being typically of the order of several N m^{-1}, i.e. of the order of the stiffness of atomic bonds. There is no other option than associating this additional flexibility of the system with the flexibility of the tip. This inherent feature has long been believed not to complicate the stick–slip physics. Actually, for a true understanding of the dynamics, one must explore at least a two-mass–two-spring generalization of the Prandtl–Tomlinson model (see figure 1), with one real mass (M) accounting for the combined inertia of the tip and cantilever, and the other effective mass (m) associated with the bending motion of the tip. Importantly, flexibility of the tip introduces an additional channel of dissipation into the system [18]. Another manifestation of the tip flexibility, as concluded from simulations of a two-spring system [22], is in the duration of slip events. Generally, a two-mass–two-spring system can exhibit a wealth of new dynamics. The key question is how small the characteristic value is for the effective mass m of the contact.

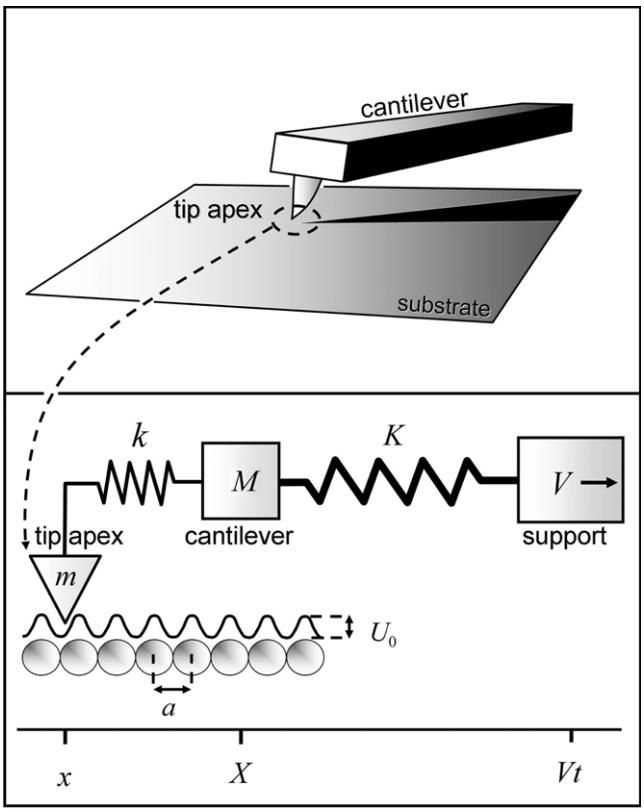

Figure 1. FFM measuring system (schematic) and the corresponding two-mass–two-spring model. K is the spring coefficient of the cantilever and k is the spring coefficient associated with the tip apex. M is the mass of the cantilever + tip system and m is an effective mass, representing the tip apex. The tip–surface interaction is modeled by a sinusoidal potential with a corrugation U_0 and with the period a of the substrate lattice. The system is driven with a constant velocity V.

According to our calculations [9], the bending deformation of an atomically sharp conical or pyramidal object (a good model for the FFM tip) is associated with only a few hundred atomic layers at its apex. This means that the effective mass $m \sim 10^{-20}$ kg, while the typical mass M of the tip–cantilever combination is about ten or more orders of magnitude higher. Taking into account the spring coefficient of the tip apex ($k \sim 1$ N m^{-1}) one finds the characteristic frequency of its bending vibration (ν_t) in the order of several GHz, while the characteristic cantilever frequencies (ν_c) fall in the kHz to MHz range. A very strong hierarchy between the effective masses and the effective frequencies involved in the problem can lead to at least two important, potentially dramatic consequences. Firstly, the low frequency response of the system as measured in FFM experiments from the motion of the cantilever can be very different from the rapid motion that is actually performed by the ultra-low effective mass, which is really probing the surface. Secondly, the role of thermal effects in the tip–surface contact can be much stronger than one could ever expect. In particular, under certain natural conditions the system can be in a strongly counterintuitive regime of friction, 'stuck in slipperiness' [9]. The cantilever shows seemingly usual atomic stick–slip, while the tip–surface contact is

completely delocalized (on the timescale of the tip–cantilever motion) due to rapid, thermally activated motion of the tip apex back and forth between the available potential wells.

The possibility of thermal contact delocalization and an ultra-low value of the effective mass m have found confirmation [10] in a good agreement between our calculations and recent high time resolution experiment [22]. The possibility of rapid activated motion of the tip apex, even at relatively high surface potential corrugations, is concerned with an ultra-high characteristic frequency of the tip apex vibrations (ν_t) which serves as 'an attempt frequency' of thermally activated jumps. In combination with generally complicated dynamics of the two-mass system motion; this necessarily leads to the prediction [11] of a multitude of physically different regimes of sliding, which represent different scenarios of energy dissipation. Besides the known regimes of *ordinary stick–slip* (SS) and *superlubricity* (SL), which take place at sufficiently high and low contact potential corrugations, respectively, there are a number of other regimes in between. *Stochastic stick–slip* (SSS) is observed under conditions when the tip apex exhibits several activated jumps back and forth between the contact potential wells, per lattice spacing passed over by the tip as a whole. Response of the tip–cantilever turns out to be somewhat different in the cases when the external spring (the cantilever) is relatively hard and soft. It follows all the jumps of the tip's apex in the former case but cannot do so in the latter. An essential difference between the cases of hard and soft external springs remains also under conditions when the contact is completely delocalized by rapid thermally activated jumps of the tip apex. The effective tip–surface interaction potential, averaged over rapid motion of the apex, remains periodic, with the period of the substrate lattice, although its corrugation is reduced with respect to the true contact potential corrugation [9]. A soft cantilever exhibits seemingly usual stick–slip motion in such a potential, in spite of an absolutely slippery contact, the regime of *stuck in slipperiness* (SinS). In contrast, for a hard cantilever this effective corrugation is not sufficient to produce mechanical instabilities and it exhibits nearly continuous sliding, with friction as low as in the case of superlubricity, the regime of *thermolubricity* (TL). One other specific situation, the *passive apex regime* (PA), arises for the contact potential corrugations slightly above the critical corrugation for the transition to superlubricity. The apex sees only one potential well for any position of the tip–cantilever, thermally activated jumps are impossible, and the apex and the tip as a whole move simultaneously. Nevertheless, the combined two-mass system can exhibit mechanical instabilities leading to the mean friction force which is very low but slightly larger than in the case of true superlubricity.

Below we will show how all these regimes manifest themselves in the temperature dependence of atomic scale friction.

3. Theoretical approach

Generally, the two-mass–two-spring system (see figure 1) is described by two coupled equations of motion, e.g. of the Langevin type, one for the cantilever + tip combination (position X and mass M) and the other for the tip apex (position x and effective mass m) moving with respect to X. Since $m \lll M$, and there is a great difference between the two characteristic timescales involved, full description of the system is problematic for computational reasons. Instead, we use a hybrid numerical description that combines a numerical solution of the Langevin equation for the full cantilever motion with a Monte Carlo simulation of the thermally activated motion of the tip's apex. This enables one to follow, nearly completely, the dynamic interplay between the rapid motion of m and the slow motion of M.

Assuming for simplicity a one-dimensional geometry and a sinusoidal tip–surface interaction, $U_s = \frac{U_0}{2}[1 - \cos(\frac{2\pi x}{a})]$, with corrugation U_0 and the substrate lattice period a, the total potential energy of the system can be written as

$$U(X, x, t) = \frac{K}{2}(Vt - X)^2 + \frac{k}{2}(X - x)^2 + U_s(x). \quad (1)$$

Here X and x are the coordinates of the cantilever and the tip apex, respectively; Vt is the position of the support that moves with the scanning velocity V; K and k denote the stiffness of the cantilever and of the tip (apex). Instantaneous lateral force between support and cantilever, as measured in experiments, is given by $F = -K(Vt - X)$, while the mean friction force is its time average.

If $m \lll M$, and hence there is a strong hierarchy of the characteristic frequencies of the tip apex (ν_t) and the cantilever (ν_c), $\nu_t \gg \nu_c$, the description can be simplified by averaging over the rapid thermal motion of the apex around 'lattice positions' x_i. For each position of the cantilever X, the $x_i(X)$ correspond to the local minima in the total potential (1) as a function of x. The number of wells available to the apex is determined by the Tomlinson-like parameter [9] $\gamma = \frac{2\pi^2 U_0}{ka^2}$. If $\gamma > 1$, there are two or more wells. This is the origin of stick–slip motion, and this also introduces the possibility of thermally activated jumps of the tip apex between the wells. Here, we restrict ourselves to the simplest approximation to the jump rate,

$$r_{ij} = r_0 \exp\left(-\frac{U_{ij}}{k_B T}\right), \quad (2)$$

assuming the prefactor $r_0 = \nu_t$ (transition state theory approximation) with the tip frequency ν_t determined by the second derivative of the total potential (1) in the vicinity of x_i, and with $U_{ij}(X)$ the potential barrier between wells i and j. Exploring a Monte Carlo algorithm for transitions of the tip apex between positions x_i and x_j with rate r_{ij}, one can describe motion of the cantilever by solving numerically only a single Langevin-type equation for M,

$$M\ddot{X} = -k\,[X - x_i(X)] - K(X - Vt) - M\eta\dot{X} + \xi. \quad (3)$$

The random force ξ is normalized as $\langle \xi(t)\xi(t') \rangle = 2M\eta_n k_B T \delta(t - t')$. According to the fluctuation-dissipation theorem for a particle interacting with a bath, $\eta_n = \eta$. In our case, damping of the cantilever motion, η, is due to its indirect coupling to the bath, via motion of the tip apex with respect to the cantilever and with respect to the surface (damping in the cantilever can be neglected [22]). The possible roles

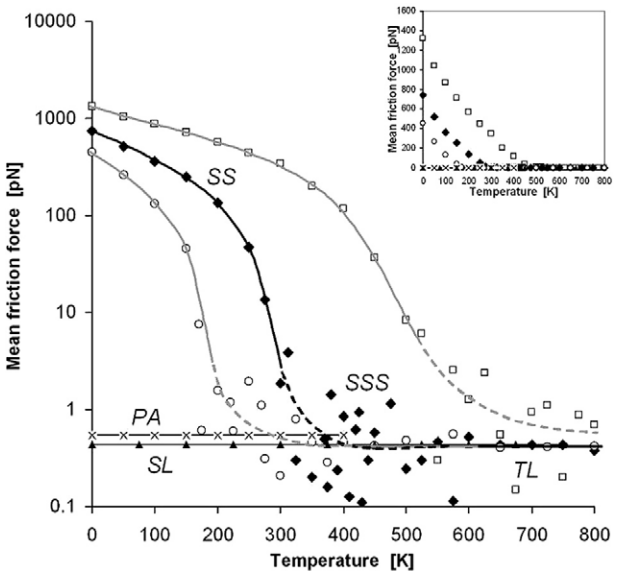

Figure 2. Mean friction force as a function of temperature, for $K = 60$ N m^{-1} (hard external spring) and for different potential corrugations: $U_0 = 0.8$ eV (□), 0.5 eV (♦), 0.35 eV (○), 0.058 eV (×), and 0.04 eV (▲). System parameters used in calculations: $k = 3$ N m^{-1}, $a = 0.25$ nm, $V = 10$ nm s^{-1}, $M = 1 \times 10^{-9}$ kg, and $m = 1 \times 10^{-20}$ kg. All friction forces have been averaged over a sliding distance of 10 lattice spacings. The lines are meant to guide the eye. Thermal noise on the cantilever motion has been switched off. Different regimes of friction are indicated: ordinary stick–slip (SS), stochastic stick–slip (SSS), stuck in slipperiness (SinS), thermolubricity (TL), passive apex regime (PA) and superlubricity (SL). The inset shows the behavior of the friction force on a linear scale.

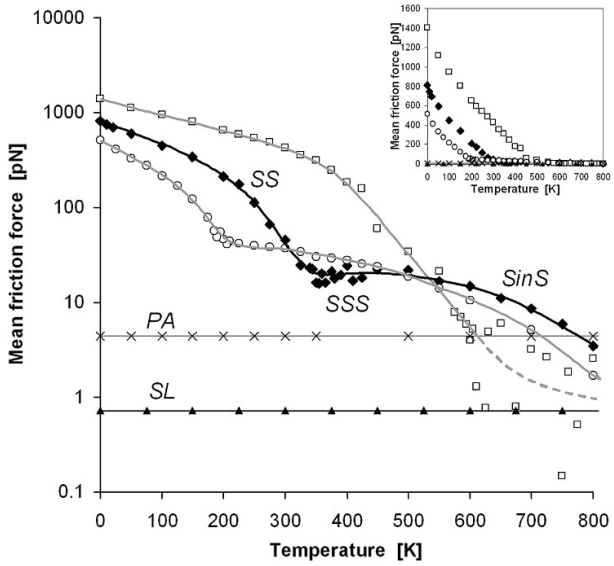

Figure 3. Similar to figure 2, but for a soft cantilever with a spring coefficient of $K = 6$ N m^{-1}. Crosses (×) correspond to potential corrugation of $U_0 = 0.05$ eV. All other parameters are as in figure 2.

of damping and thermal noise on the cantilever have been discussed earlier [11]. We have checked that of a wide range $0.1\,\nu_c < \eta < 10\,\nu_c$ the results for the mean friction force do not change considerably, although the instantaneous lateral force exhibits stronger fluctuations at lower damping and higher random force amplitude, as expected. The particular results presented below (figures 2–5) correspond to the case of slightly underdamped motion, $\eta = 0.8\,\nu_c$, while thermal noise on the cantilever has been artificially switched off by taking $\eta_n = 0$, in order to better visualize the inherent dynamics of the system under interest.

Note that the simple approximation for the jump rate prefactor in (2), $r_0 = \nu_t$, tacitly implies a moderate damping of the tip apex motion, and this is the only principal physical assumption made above. Generally, as follows from Kramers-like theories of activated processes [23], the prefactor depends on the particle's coupling to the bath; in our case this suggests dependence of r_0 on damping of the tip apex motion with respect to the cantilever (η_{ac}) and with respect to the surface (η_{as}). The traditional, transition state theory approximation used here corresponds to the case when $\max\{\eta_{ac}, \eta_{as}\} \sim \nu_t$.

An additional restriction is concerned with the discrete jump picture implied in (2), which is justified when the barriers between relevant potential wells are high with respect to $k_B T$. The results of calculations presented below correspond to sufficiently high (actually very typical) potential corrugations $U_0 > 0.3$ eV, for which the discrete description of the tip apex motion remains justified over a wide range of temperatures considered. For comparison, temperature-independent results for very low potential corrugations will also be presented, for the case when $\gamma < 1$ and there are no activated jumps of the tip apex at all.

4. Temperature dependence of atomic scale friction

The behavior of the mean friction force as a function of temperature is shown in figures 2 and 3 for different contact potential corrugations and for two cases of relatively hard ($K = 60$ N m^{-1}) and soft ($K = 6$ N m^{-1}) external springs, respectively. Both cases are typical for modern experiments [12–14, 22]. Calculations have been performed for very typical values of all the other system parameters involved: tip stiffness $k = 3$ N m^{-1}, substrate lattice spacing $a = 0.25$ nm, scanning velocity $V = 10$ nm s^{-1}, the cantilever mass $M = 1 \times 10^{-9}$ kg. The effective mass of the contact has been taken as $m = 1 \times 10^{-20}$ kg, as calculated in [9]. The friction force has been averaged over a sliding distance of ten substrate lattice spacings passed over by the tip.

As expected [11], the behavior of the system turns out to be qualitatively different for the hard (figure 2) and soft (figure 3) external springs, in view of different responses of the cantilever to thermally activated motion of the tip apex. For a softer cantilever, its reaction time is somewhat larger, and the distance is essentially larger between its equilibrium positions corresponding to different lattice positions of the apex.

In both cases, one observes decreasing friction with increasing temperature, provided the contact potential corrugation is not too small. Clearly, when two or several surface wells are accessible for the tip apex ($\gamma > 1$), its thermally activated jumps between the wells, more frequent at higher

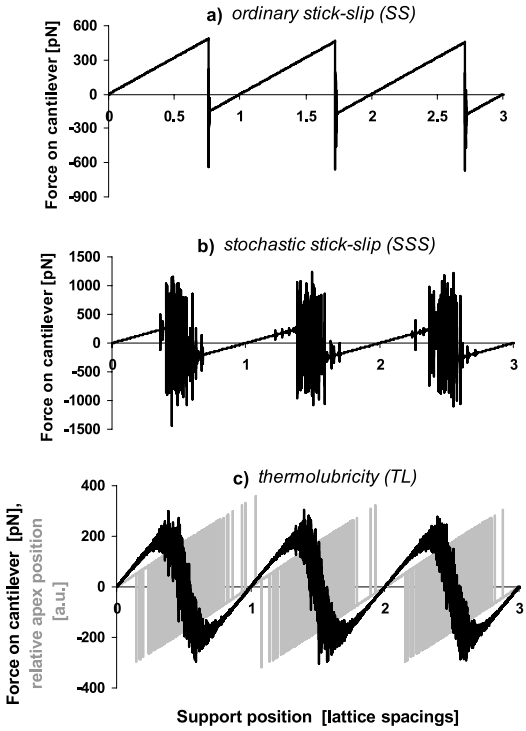

Figure 4. Lateral force between the cantilever and support as a function of its position, Vt/a, for a hard external spring with $K = 60$ N m^{-1}, potential corrugation $U_0 = 0.5$ eV, and all other parameters as in figure 2. Calculation results are shown for temperatures 200 K (a), 350 K (b) and 700 K (c). Corresponding friction regimes are indicated. Thermal noise on the cantilever motion has been switched off in order to better visualize the inherent dynamics of the system. In panel (c), the positions of the tip apex relative to the support, $(Vt - x)/a$, are also shown to demonstrate thermal contact delocalization (gray lines). Note that the time resolution in the plotted tip apex positions is too coarse for displaying all calculated jumps.

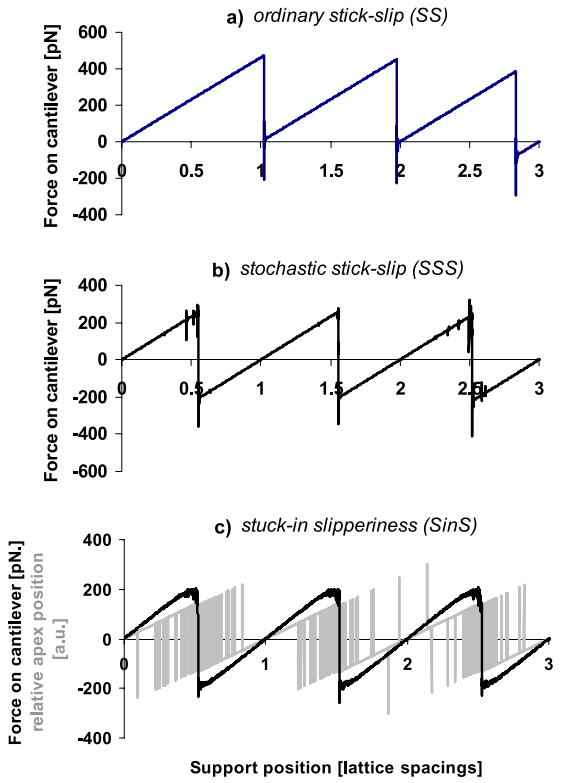

Figure 5. Similar to figure 4, but for a soft cantilever with a spring coefficient of $K = 6$ N m^{-1}. Calculation results are shown for $U_0 = 0.5$ eV and for temperatures 200 K (a), 350 K (b) and 700 K (c).

temperatures, effectively 'smooth' the contact. This is in contrast to temperature-independent results at very low corrugations, when only one well is seen by the apex for any position of the support ($\gamma < 1$) and thermal activation does not take place. Besides these features, that could be anticipated, there are really nontrivial results.

Thus, one observes that thermal effects can be very strong, especially in the case of a hard cantilever. For instance, for the surface corrugation $U_0 = 0.5$ eV, in a temperature range slightly below 300 K (see figure 2) a modest change of T by several tens degrees causes an order-of-magnitude change of friction; for $U_0 = 0.35$ eV the corresponding temperature range is met below 200 K. Clearly, such a strong 'thermal lubrication' is related to a huge value of the attempt frequency of activated jumps of the tip apex, as a consequence of its ultra-low effective mass.

Even more surprising is alternation of the temperature intervals with stronger and weaker variation of the friction force. The nontrivial shape of the curves $F_{\text{friction}}(T)$, in the cases of both figures 2 and 3, indicate transitions between different regimes of sliding corresponding to different scenarios of energy dissipation.

Maybe most unexpected, at first glance at least, are the strong fluctuations of the friction force seen in certain intervals of temperature, in spite of averaging over a relatively long distance passed along the surface (ten lattice spacings in our case). For instance, for the hard external spring and $U_0 = 0.5$ eV, an unstable friction force is met in a temperature range between 300 and 600 K, where it varies—from one run to the other—over more than one order of magnitude, while at lower and higher temperatures, friction is stable (see figure 2). Also counterintuitive is that stronger fluctuations are observed for the harder cantilever but not for the softer one (compare figures 2 and 3). For higher potential corrugations the range of instability is seen to move towards higher temperatures.

One other counterintuitive observation is concerned with the crossover between the curves in figure 3, the case of soft cantilever. Friction can be stronger for weaker potential corrugation (i.e. for a smoother contact), as for instance for $U_0 = 0.35$ eV with respect to 0.5 eV in a temperature range around 400 K. This effect has already been met and explained in our previous work [11].

All the features summarized above are concerned with a multitude of different regimes of friction [11] and transitions between them with changing temperature. We can visualize these regimes, since, within the computational scheme used by us, one can follow both the slow motion of the friction sensor M (that is recorded in FFM experiments) and the rapid dynamics of the effective mass m which is actually probing the substrate. As illustrated in figure 4, in the

case of a hard external spring, the decrease of friction with increasing temperature is accompanied by transitions from *ordinary stick–slip* (SS) to *stochastic stick–slip* (SSS) and then to *thermolubricity* (TL). In the case of a soft cantilever (figure 5), the system goes from SS to SSS and then to *stuck in slipperiness* (SinS).

If the contact potential corrugation is not too small, any system at sufficiently low temperatures is in the ordinary stick–slip regime; see figures 4(a) and 5(a). In this case, as seen from the insets to figures 2 and 3, friction force decreases nearly linearly with temperature increase. The physics behind is simply the same as discussed earlier [7, 16, 17], in the framework of the one-spring Tomlinson model, with respect to the velocity dependence of the friction. Thermal activation always initiates the system to start slipping somewhat earlier than the positions of mechanical instability are reached. The new feature brought out by the two-spring model with an ultra-low effective mass of the contact is that the slipping and, hence, energy dissipation actually have two steps. First, part of energy (which has been stored in the deformed tip) is dissipated during rapid slip of the tip apex, on the timescale of $(\nu_t)^{-1}$. Then the rest of energy (stored in the cantilever) is dissipated during the slip of the cantilever, on the timescale of $(\nu_c)^{-1}$.

With increasing temperature, the behavior of the system becomes complicated by the occurrence of a number of activated jumps of the apex back and forth between the accessible potential wells, per substrate lattice period passed over by the cantilever. As seen in figure 4(b), the hard cantilever exhibits multiple slips back and forth along the surface. Each of these slips directly follows corresponding jump of the apex (not shown here). As a consequence, the mean friction force is not only very low in this regime, but it strongly fluctuates, in view of stochastic nature of thermally activated jumps. For higher potential corrugations this stochastic stick–slip regime is met at higher temperatures (see figure 2), in accordance with equation (2). In the case of a soft external spring, the manifestation of this stochastic regime is somewhat different. A soft cantilever cannot follow rapid jumps of the tip apex and exhibits single slips (see figure 5(b)), like in the ordinary stick–slip regime. The response to the jumps of the apex is seen as relatively weak fluctuations of the instantaneous force at the sticking parts of the cycle. As a consequence, fluctuations of the mean friction force are still there in this SSS regime (see figure 3), but they are more modest than in the case of a hard cantilever.

At higher temperatures the behavior changes drastically. The contact is seen to exhibit very rapid activated jumps between the accessible lattice positions (gray lines in figures 4(c) and 5(c)), thus being nearly completely delocalized on the timescale of the scanning. (Note that in view of a finite time resolution in these figures not all jumps of the apex are seen.) It comes as no surprise that the massive friction sensor is not able to follow these rapid jumps at all, but exhibits fluctuating but on average very regular behavior (black lines in figures 4(c) and 5(c)). This resulting behavior depends on the external spring stiffness (see section 2). In the case of hard cantilever, this is a continuous sliding (figure 4(c)) which leads to a very small friction force, the regime of thermolubricity. Increase of temperature in this regime results in a smoother behavior of the sensor (smaller fluctuations of the instantaneous lateral force), but has little effect on the mean friction force, as is indeed seen in figure 2. In the case of a soft external spring, the cantilever exhibits specific stick–slip motion (figure 5(c)), the regime of stuck in slipperiness. The mean friction force is not too small (in contrast to the previous case), and it decreases with further increase of temperature, as seen in figure 3. This last effect is entropic in nature [10] and it can be understood as a decrease of the corrugation of the effective tip–surface interaction averaged over rapid activated motion of the apex.

5. Concluding remarks

The results presented above have been obtained using very typical values of all the system parameters involved. The only new and essentially important ingredient is an ultra-low value of the effective mass of the nanoscale contact ($m \sim 10^{-20}$ kg) which is thus ten of more orders of magnitude smaller than the mass (M) of the macroscopic friction sensor. This is a very rapid activated motion of m and the corresponding, partial or complete, delocalization of the contact which are responsible for the puzzling behavior of friction observed. Importantly, the assumption of the low value of m is well supported. First, it has been concluded from model calculations [9], being directly related to an atomically small stiffness of FFM tips. Since in all experiments where this parameter could be controlled the value of k was in the range of several N m^{-1}, regardless of the tip material and mode of preparation, the result seems rather universal. Second, it has found a good confirmation [10] in an excellent agreement between the calculated friction force behavior and some observations of a recent, high resolution FFM experiment [22].

Our results will we hope strongly stimulate temperature-variable FFM experimentation. In fact, this work adds one other, most impressive example to a series of our recent observations [19, 9–11] that the role of thermal effects in atomic scale friction is crucial. Most importantly, there must be a rich variety of physically different friction regimes related to different types of contact delocalization, and actually they represent different scenarios of energy dissipation.

A strong variation of friction with temperature has been observed in a very recent FFM experiment [8]. Remarkably, one can find a high degree of similarity between the qualitative behavior $F_{\text{friction}}(T)$ reported [8] and our predictions shown in figures 2 and 3. More detailed, quantitative measurements are necessary for comparison between the theory and experiment. Nevertheless, at this stage, one certainly can already speculate about the manifestation of different regimes of friction in the experiment.

Although direct experimental verification of most of our observations is still lacking, one other, far-reaching speculation can be advanced. It is common belief that an FFM tip models a single nanoasperity, one of those that establish the contact between macroscopic sliding bodies. If so, our results suggest that there is a much more pronounced role of thermally driven dynamics in macroscopic sliding than has ever been imagined.

Acknowledgments

The authors are grateful to Daniel Abel and Joshua Dijksman for significant contributions and substantial help in the early stages of this investigation. This work is part of the research program of the Stichting voor Fundamenteel Onderzoek der Materie (FOM) and was made possible by financial support from the Nederlandse Organisatie voor Wetenschappelijk Onderzoek (NWO).

References

[1] Mate C, McClelland G, Erlandsson R and Chiang S 1987 *Phys. Rev. Lett.* **59** 1942
[2] Persson B N J 1998 *Sliding Friction: Physical Principles and Applications* (Berlin: Springer)
[3] Carpick R W and Salmeron M 1997 *Chem. Rev.* **97** 1163
[4] Urbakh M, Klafter J, Gourdon D and Israelachvili J 2004 *Nature* **430** 525
[5] Prandtl L 1928 *Z. Angew. Math. Mech.* **8** 85
[6] Tomlinson G A 1929 *Phil. Mag.* **7** 905
[7] Gnecco E, Bennewitz R, Gyalog T, Loppacher Ch, Bammerlin M, Meyer E and Güntherodt H-J 2000 *Phys. Rev. Lett.* **84** 1172
[8] Zhao X, Hamilton M, Sawyer W G and Perry S S 2007 *Tribol. Lett.* **27** 113
[9] Krylov S Yu, Dijksman J A, van Loo W A and Frenken J W M 2006 *Phys. Rev. Lett.* **97** 166103
[10] Abel D, Krylov S Yu and Frenken J W M 2007 *Phys. Rev. Lett.* **99** 166102
[11] Krylov S Yu and Frenken J W M 2007 *New J. Phys.* **9** 398
[12] Dienwiebel M, Verhoeven G S, Pradeep N, Frenken J W M, Heimberg J A and Zandbergen H W 2004 *Phys. Rev. Lett.* **92** 126101
[13] Socoliuc A, Bennewitz R, Gnecco E and Meyer E 2004 *Phys. Rev. Lett.* **92** 134301
[14] Dienwiebel M, Pradeep N, Verhoeven G S, Zandbergen H W and Frenken J W M 2005 *Surf. Sci.* **576** 197
[15] Müser M H, Urbakh M and Robbins M O 2003 *Adv. Chem. Phys.* **126** 187
[16] Sang Y, Dube M and Grant M 2001 *Phys. Rev. Lett.* **87** 174301
[17] Dudko O K, Filippov A E, Klafter J and Urbakh M 2002 *Chem. Phys. Lett.* **352** 499
[18] Reimann P and Evstigneev M 2004 *Phys. Rev. Lett.* **93** 230802
[19] Krylov S Yu, Jinesh K B, Valk H, Dienwiebel M and Frenken J W M 2005 *Phys. Rev.* E **71** 065101(R)
[20] Fusco C and Fasolino A 2005 *Phys. Rev.* B **71** 045413
[21] Socoliuc A, Gnecco E, Maier S, Pfeiffer O, Baratoff A, Bennewitz R and Meyer E 2006 *Science* **313** 207
[22] Maier S, Sang Yi, Filleter T, Grant M, Bennewitz R, Gnecco E and Meyer E 2005 *Phys. Rev.* B **72** 245418
[23] Hänggi P, Talkner P and Borkovec M 1990 *Rev. Mod. Phys.* **62** 251